# Transfer hydrogenolysis of aromatic ethers promoted by the bimetallic Pd/Co catalyst

F. Mauriello[1,*], H. Ariga-Miwa[2], E. Paone[1], R. Pietropaolo[1], S. Takakusagi[2], and K. Asakura[2,*]

[1] *Dipartimento DICEAM, Università Mediterranea di Reggio Calabria, Loc. Feo di Vito, I-89122 Reggio Calabria, Italy*

[2] *Institute of Catalysis, Hokkaido University, Kita-ku N21W10, Sapporo, Hokkaido 001-0021, Japan*

**Corresponding authors.*

*Tel: +39-0965-1692278; Fax: +39-0965-1692201*
*E-mail: francesco.mauriello@unirc.it. (F. Mauriello)*

*Tel: +81-11-7069113; Fax: +81-11-7069113*
*E-mail: askr@cat.hokudai.ac.jp (K. Asakura)*

**Keywords:** transfer hydrogenolysis; lignin, aromatic ethers; heterogeneous catalysis; palladium; cobalt bimetallic Pd-Co catalyst

**Abstract**

The transfer hydrogenolysis of lignin derived aromatic ethers (benzyl phenyl ether, phenethyl phenyl ether and diphenyl ethers) have been investigated by using the coprecipitated Pd/Co as heterogeneous catalyst and 2-propanol as H-donor/solvent. A quantitative conversion of benzyl phenyl ether into toluene and cyclohexanol was obtained after 180 minutes at 240 °C. The bimetallic Pd/Co catalyst is, by far, more efficient if compared to commercial Pd/C and Co-based catalytic systems showing, at the same time, an excellent reusability. The enhanced ability in the C-O bond cleavage in aromatic ethers is related to the formation of bimetallic Pd-Co ensembles, arisen from the preparation procedure adopted, as confirmed by a complete physico-chemical characterization that includes XRD, SEM, TEM, $H_2$-TPR, XPS and EXAFS analysis.

## 1. Introduction

The use of lignocellulosic biomasses for the sustainable production of renewable energy, fuels and chemicals is unquestionably known [1-3]. The key constituents of lignocellulose (cellulose, hemicellulose and lignin) are characterized by a chemical structure that can provide starting substrates for the preparation of a huge variety of building block chemicals. Cellulose and hemicellulose can be first depolymerized into C6-C5 sugars and then converted into short-chain alcohols, polyols, esters and acids [4]. On the other hand, lignin is the only lignocellulosic component that allows the production of bio-based aromatic compounds [5]. Renewable aromatics will constitute a significative quota of the future global bioeconomy due to their wide-ranging industrial applications including polymers, textiles, paints, tires, coatings, fragrances and pharmaceuticals [6].

One of the most adopted chemical approaches to lignin depolymerization is surely the hydrogenolysis technique (the direct C-O bond cleavage by means of molecular $H_2$) that, allowing also the efficient reduction of the oxygen content in lignocellulosic constituents and their chemical derivatives, is becoming one of the core technologies in the modern bio-refinery [7]. Therefore, the basic chemistry of C-O bond breaking of aromatic ethers is still one the fundamental task to accomplish in order to selective produce chemicals from lignin [8].

However, in hydrogenolysis reactions, the "lysis" of carbon–carbon or carbon–heteroatom bonds is generally promoted by homogeneous or heterogeneous catalysts in presence of high-pressure molecular hydrogen ($H_2$ is poorly soluble in most reaction solvents) with all associated problems including security hazards, expensive infrastructures, purchase and transport of the explosive gas.

In the last years, a significant growth to an alternative catalytic approach avoiding the direct use of molecular hydrogen was observed [9, 10]. To this regard, the catalytic transfer hydrogenolysis (CTH) may represent a valid green alternative to classic hydrogenation/hydrogenolysis reactions owing to the use of indirect H-source molecules [11]. Simple organic molecules including short chain alcohols (2-propanol, ethanol and methanol) and acids (formic acid) can be efficiently used as H-donor for CTH

reactions. At the same time, CTH molecules are generally easily to handle, potentially obtainable from renewable feedstocks and, due to their lower tendency to release hydrogen, may allow a higher production of aromatic compounds from lignin and its derived molecules.

In the last years, several authors used different homogeneous and heterogeneous catalysts for the hydrogenolysis and transfer hydrogenolysis of lignin and lignin-derived ethers [12-18]. In particular, the commercial Pd/C has attracted a lot of research interests allowing an efficient transformation of lignin and of a variety of aromatic ethers using formic acid and 2-propanol as H-donors [19-21].

Nevertheless, the introduction of a second metal has been found helpful to increase the catalytic performances [22-24]. For instance, the addition of iron to palladium, through the co-precipitation technique, produces intimate metal-support interactions that create a synergistic effect enabling a higher reactivity in several important reactions including the CTH of aromatic ethers [25-29]. In recent years, we investigated the CTH of glycerol also by using the co-precipated Pd/Co catalyst under mild operating conditions [30-32]. This catalyst was found to be definitely the most efficient coprecipitated Pd catalysts in the C-O bond cleavage in biomass derived polyols.

In this paper, we evaluate the performance of the co-precipitated Pd/Co catalyst in the CTH of benzyl phenyl ether (BPE), 2-phenethyl phenyl ether (PPE) and diphenyl ether (DPE) that represent the simplest lignin-derived aromatic ethers and can be used to mimic catalytic cleavage of the most common lignin linkages (Scheme 1). A physisco-chemical characterization by means of XRD, SEM-EDX, TEM, $H_2$-TPR, XPS and EXAFS analysis highlights the presence of bimetallic Pd-Co ensembles that positively promote the C-O bond cleavage of the investigated aromatic ethers. If compared with commercial Pd/C and other benchmark cobalt-based systems (metallic Co, CoO and $Co_3O_4$), the bimetallic Pd/Co catalyst shows higher activity. Moreover, the Pd/Co catalyst can be recycled up to six times without any activity loss and easily recovered from the reaction medium magnetically.

Scheme 1 about here

## 2. Experimental Section

### 2.1 Catalysts preparation

2-Phenethyl phenyl ether (PPE) was purchased from Frinton Laboratories (USA). All other chemicals were purchased from Carlo Erba reagent and used without further purification.

The Pd/Co catalyst (with nominal palladium loading of 5 wt%) was prepared through the co-precipitation technique. An aqueous solution of palladium (II) nitrate and cobalt (II) nitrate hexahydrate was added dropwise into an aqueous solution of $Na_2CO_3$ (1M). The obtained catalyst was filtered, washed with deionized water until neutral pH was reached and dried overnight at 120°C. The obtained solid was then oxidized at 300°C for 3 hours under an air flow and, before use, reduced at 300°C for 2 h under a hydrogen flow.

### 2.2 Catalysts Characterization.

XRD data were acquired at room temperature on a Bruker D2 PHASER diffractometer by using the Ni β-filtered Cu Kα radiation (λ=0.15418 nm) in the 2θ range of 20–80° at a scan speed of 0.5°$min^{-1}$.

XRF analysis were performed with a Bruker Tracer IV-SD Spectrometer (Bruker, Germany) at 40 keV, 15 μA over 15 s with peak assignment based on alignment with K-line energy transitions.

SEM-EDX analysis were carried out on a Phenom Pro-X scanning electron microscope (SEM) equipped with an energy-dispersive X-ray (EDX). EDX analysis was used in order to evaluate the content and the dispersion of metals, acquiring, for all samples, at least 20 points for 3 different magnifications.

The particle size and the relative morphology of investigated catalysts were analysed by performing Transmission Electron Miscroscopy (TEM) measurements using a JEM-2100F (JEOL, Japan) operating at an acceleration voltage of 200 kV and directly interfaced with a computer controlled-CCD for real-time image processing. Particle size distributions were obtained by counting several hundred particles

visible on the micrographs on each sample. From the size distribution, the average diameter was calculated by using the expression: $d_n = \Sigma n_i d_i / n_i$ where $n_i$ is the number of particles of diameter $d_i$.

$H_2$-TPR measurements were performed using a conventional TPR apparatus. The dried samples (50mg) were heated at a linear rate of 10 °C $min^{-1}$ from 0 to 1000 °C in a 5vol % of $H_2$/Ar mixture at a flow rate of 20 $cm^3$ $min^{-1}$. $H_2$ consumption was monitored with a thermal conductivity detector (TCD).

XPS measurements were performed on a JPS-9010MC photoelectron spectrometer using an Al Kα (1486.6 eV) radiation source. After the reduction treatment, samples were introduced into the XPS chamber, avoiding exposure to air. All spectra were recorded at room temperature, and the binding energies (BE) were set taking the C 1s peak at 284.6 eV as reference. Pd/Co sample was also recorded after an additional "in situ reduction" condition (denoted as "in situ-reduced") in an auxiliary reaction chamber at 200 °C under 100 Pa $H_2$ for 4 h.

Extended X-ray absorption fine structure (EXAFS) of the Pd-based catalysts were measured at the Photon Factory of the High Energy Accelerator Research Organization - KEK (Tsukuba, Japan) . Co-K and Fe-K edge XANES/EXAFS spectra for the catalysts were obtained using a Si(111) two-crystal monochromator with beam line BL9A and Pd K-edge spectra were obtained using a Si(311) two-crystal monochromator with beam line NW10A. Analysis of the EXAFS data was performed using the EXAFS analysis program, REX (Rigaku Co.).

**2.3 Catalytic Tests.**

Reactions were carried out in a 100 ml stainless steel autoclave at a stirring speed of 500 rpm. The reactor, loaded with the reduced catalyst (0.125 g) suspended in a 0.1 M solution of the chosen substrate in 2-propanol (40 mL) was purged three times with $N_2$ (99.99%) and subsequently pressurized at the desired gas ($N_2$ or $H_2$) pressure and heated up at the chosen reaction temperature. At the end of each reaction, the system was cooled and, when at room temperature, the pressure was released carefully and the liquid phase analyzed using an off-line gas chromatograph (Agilent 6890N equipped with CP-WAX 52CB, 60 m, i.d. 0.53 mm).

With respect to recycling tests, after any run, the catalyst was recovered, carefully washed with 2-propanol, and reused under the same reaction conditions.

The conversion, product selectivity and product yield in the liquid phase were calculated on the basis of the following equations:

$$\text{Conversion [\%]} = \frac{\text{mol of reacted substrate}}{\text{mol of substrate feed}} \times 100 \quad (1)$$

$$\text{Liquid phase selectivity [\%]} = \frac{\text{mol of specific product in liquid phase}}{\text{sum of mol of all products in liquid phase}} \times 100 \quad (2)$$

$$\text{Product Yield [\%]} = \frac{\text{mol of specific product}}{\text{mol of substrate feed}} \times 100 \quad (3)$$

## 3. Results and Discussion

### 3.1 Catalyst preparation and characterization

The Pd/Co catalyst was prepared through the co-precipitation of palladium nitrate and cobalt nitrate hexahydrate, simultaneously added dropwise into a 1 M aqueous solution of $Na_2CO_3$. The precipitated solid was filtered, washed with distilled water until a neutral pH was reached, dried overnight at 120°C, calcinated at 300°C in air and finally reduced under a flow of molecular hydrogen at 300°C. The main characteristic of the Pd/Co catalyst are reported in Table 1.

Table 1 about here

Figure 1 about here

The X-ray powder diffraction (XRD) pattern of the unreduced Pd/Co catalyst shows diffraction peaks typical of pure cubic crystalline $Co_3O_4$ (Figure 1, up) [33]. After reduction, diffraction peaks of metallic cobalt can be easily observed indicating the promoting effect of Pd in the support reduction (Figure 1,

down). This point is worth of remark since the complete reduction of $Co_3O_4$ into metallic Co in $H_2$ atmosphere generally occurs up to 400°C [34].

Highly dispersed palladium particles are easily detected by SEM-EDX analysis (Figure 2) [35].

Figure 2 about here

The average Pd particles size and the relative distribution were determined by using the TEM tecnique. Representative TEM images of reduced Pd/Co catalyst are reported in Figure 3 where Co metal particles and Pd ensembles with a broad particles size distribution of about 8.7 nm was measured.

Figure 3 about here

The $H_2$-TPR profile of the Pd/Co sample is characterized by only one broad and intense peak cantered at about 260°C that can be related to the simultaneous reduction of both palladium and cobalt cations (Figure 4). Most important, the $H_2$-TPR profile of Pd/Co (Figure 4) is very similar to that of the $Co_3O_4$ sample prepared by the identical synthetic procedure although the main reduction peak is shifted to lower temperatures of about 150°C. This phenomenon is well known and is commonly ascribed to the promoting effect of well-dispersed palladium particles on the $Co_3O_4$ reduction indicating a strong interaction between Pd ions and the metal oxide support [36].

Figure 4 about here

The XPS spectrum of the reduced Pd/Co catalyst shows that the binding energy of the Pd $3d_{5/2}$ level appears at about 0.5 eV value higher than that of the binding energy of metallic palladium, indicating the presence of partial positively charged Pd species, suggesting the formation of a Pd-Co alloy (Figure

5) [37-38]. At the same time, the binding energy of Co $2p_{3/2}$ is characterized by a sharp peak typical of metallic Co [39].

Figure 5 about here

Table 2 reports the main results of extended X-ray absorption fine structure (EXAFS) characterization at the Pd K-edge. In the Pd/Co catalyst, the most marked feature is the direct observation of a shorter scattering Pd-Co path of 2.51 Å compared with the Pd–Pd distance of about 2.70 Å, confirming the formation of Pd-Co bimetallic ensembles [40].

Table 2 about here

**3.2 Catalytic tests**

The catalytic results of Pd/Co and Pd/C catalysts, in the transfer hydrogenolysis of BPE, are reported in Table 3.

Table 3 about here

The Pd/Co catalyst shows an excellent activity showing, after 3 hours of reaction, a high BPE conversion at 210°C (88%) and a total conversion (100%) at 240°C.

The distribution pattern of products, was found to change within the investigated temperature range. Indeed, at the lower temperature (180°C), the only reaction products observed are toluene (Tol) and phenol (Phe). When the temperature increases, phenol is progressively converted into cyclohexanol (CXO) becoming, at 240°C, the main reaction product together with toluene. Although at high reaction temperatures, the aromatic yield drops to 50%, it is worth to highlight that cyclohexanol is an important

feedstock in the industrial chemistry being used as a precursor to nylons, plastics, detergents and insecticides.

On the contrary, the commercial Pd/C exhibits a significant lower activity. Indeed, at 210°C the BPE conversion is less than 20% and the maximum is 45% at 240°C, the highest temperature investigated (Table 1). The modest performance of the commercial Pd/C catalyst in CTH reactions was already reported and attributed to its lower ability to dehydrogenate 2-propanol [26, 30].

Furthermore, pure metallic cobalt, CoO and $Co_3O_4$ were tested within the same temperature range and no BPE conversion was found, clearly indicating that palladium presence in the catalyst is essential for the C–O bond breaking. The lack of any noteworthy reactivity using either Pd/C or Co-based catalysts, confirms that the marked activity shown by the bimetallic Pd/Co catalyst has to be attributed to the strong interaction between palladium and cobalt, as consequence of the preparation method (co-precipitation) in analogy with other reports attaining to glycerol hydrogenolysis.

The CTH of BPE was also investigated at different reaction times (Figure 6) at 210°C (the best reaction temperature that maximizes aromatic production). The BPE conversion was completed after 6 h of reaction, and toluene yields progressively increase on increasing reaction times, reaching a maximum value at 360 min. Furthermore, its hydrogenation into methylcyclohexane was not registered. Comparatively, phenol reaches the highest yield value at 180 min and then progressively decreases because of further hydrogenation into cyclohexanol.

Figure 6 about here

On the other hand, the reusability of Pd/Co catalyst was subsequently evaluated under the harsh reaction condition adopted (240°C for 3 hours). Pd/Co maintains its high activity after six consecutive recycling runs and no changes in product selectivity was found, highlighting the good stability of the catalyst (Figure 7).

Figure 7 about here

The substrate scope was subsequently extended to additional aromatic ethers representative of lignin linkages, namely, PPE and DPE both under CTH conditions as well as under classical hydrogenolysis conditions (Figure 8). Catalytic tests show that: (i) improved conversions can be easily achieved in presence of molecular hydrogen and (ii) the cleavage of C-O bond of PPE and DPE is less efficient due to the higher bond dissociation energies (β-O-4 = 289 kJ/mol and 4-O-5 = 314 kJ/mol) involved [42, 43].

Figure 8 about here

## 4. Conclusions

The catalytic conversion of lignin-deriving aromatic ethers (benzyl phenyl ether, 2-phenethyl phenyl ether and diphenyl ether) was investigated under transfer hydrogenolysis conditions over the bimetallic Pd/Co catalyst by using 2-propanol as solvent/H-donor.

Bimetallic Pd/Co catalysts, prepared by the coprecipitation technique, are able to effectively cleave the C−O bond of benzyl phenyl ether (α-O-4 lignin model molecule) that, after 3 hours at 240°C, is selectively converted into toluene and cyclohexanol. Six consecutive recycling tests in the transfer hydrogenolysis of BPE proved the good stability of the Pd/Co catalyst that can be easily recoverable magnetically from the reaction medium.

The CTH of 2-phenethyl phenyl ether and diphenyl ether were found to be less efficient due to the higher bond dissociation energies involved in the C-O bond breaking.

Physicochemical characterizations clearly demonstrate to the presence of bimetallic Pd/Co ensembles (alloy-type) as a crucial factor involved in the observed enhancement of the catalytic activity.

## References


[1] M. Besson, P. Gallezot, C. Pinel, Chem. Rev. 114 (2014) 1827−1870.

[2] C.O. Tuck, E. Peréz, I.T. Horvaťh, R.A. Sheldon, M. Poliakoff, Science 337 (2012) 695−699.

[3] C.-H. Zhou, X. Xia, C.-X. Lin, D.-S. Tong, J. Beltramini, Chem. Soc. Rev. 40 (2011) 5588−5617.

[4] I. Delidovich, K. Leonhard, R. Palkovits, Energy Environ. Sci. 7 (2014) 2803-2830.

[5] C. Xu, R. A. D. Arancon, J. Labidi, R. Luque, Chem. Soc. Rev. 43 (2014) 7485−7500.

[6] OECD (2014), "Biobased Chemicals and Bioplastics: Finding the Right Policy Balance", OECD Science, Technology and Industry Policy Papers, No. 17, OECD Publishing. http://dx.doi.org/10.1787/5jxwwfjx0djf-en

[7] A. M. Ruppert, K. Weinberg, R. Palkovits, Angew. Chem., Int. Ed. 51 (11) (2012) 2564−2601.

[8] M. Zaheer, R. Kempe, ACS Catal. 5 (2015) 1675−1684.

[9] D. Wang, D. Astruc, Chem. Rev. 115 (13) (2015) 6621−6686.

[10] M. J. Gilkey, E. X. Bingjun, ACS Catal. 6 (2016) 1420−1436.

[11] C. Espro, B. Gumina, T. Szumelda, E. Paone, F. Mauriello, Catalysts, 8 (8) (2018) 313.

[12] A. G. Sergeev, J. F. Hartwig, Sciencec332 (2011) 439−443.

[13] X. Wang, R. Rinaldi, Energy Environ. Sci. 5 (8) (2012) 8244−8260.

[14] X. Wang, R. Rinaldi, Angew. Chem., Int. Ed. 52 (2013) 11499−11503.

[15] G. S. Macala, T. D. Matson, C. L. Johnson, R. S. Lewis, A. V. Iretskii, P. C. Ford, ChemSusChem 2 (2009) 215−217.

[16] K. Barta, T. D. Matson, M. L. Fettig, S. L. Scott, A. V. Iretskii, P. C. Ford, Green Chem. 12 (2010) 1640−1647.

[17] F. Mauriello, E. Paone, R. Pietropaolo, A.M. Balu, R. Luque, ACS Sustain Chem Eng 6 (7) (2018) 9269–9276.

[18] M. Guo, J. Peng, Q. Yang, C. Li, ACS Catal. 8 (2018) 11174–11183.

[19] M. V. Galkin, S. Sawadjoon, V. Rohde, M. Dawange, J. S. M. Samec, ChemCatChem 6 (1) (2014) 179−184.

[20] M. V. Galkin, J. S. M. Samec, ChemSusChem 7 (8) (2014) 2154− 2158.

[21] M. V. Galkin, C. Dahlstrand, J. S. M. Samec, ChemSusChem 8 (2015) 2187−2192.

[22] D.M. Alonso, S.G. Wettstein, J.A. Dumesic, Chem. Soc. Rev. 41 (2012) 8075–8098.

[23] J.-w. Zhang, Y. Cai, G.-p. Lu, C. Cai, Green Chem. 18 (2016) 6229−6235.

[24] J. Zhang, J. Teo, X. Chen, H. Asakura, T. Tanaka, K. Teramura, N. Yan, ACS Catal. 4 (2014) 1574−1583.

[25] C. Espro, B. Gumina, E. Paone, F. Mauriello, Catalysts 7 (2017) 78.

[26] E. Paone, C. Espro, R. Pietropaolo, F. Mauriello, Catal. Sci. Technol. 6 (22) (2016) 7937−7941.

[27] B. Gumina, F. Mauriello, R. Pietropaolo, S. Galvagno, C. Espro, Molecular Catalysis, 446 (2018) 152–160.

[28] D. Cozzula, A. Vinci, F. Mauriello, R. Pietropaolo, T.E. Müller, ChemCatChem 8 (2016) 1515–1522.

[29] M.G. Musolino, L.A. Scarpino, F. Mauriello, R. Pietropaolo, Green Chem. 11 (2009) 1511–1513.

[30] F. Mauriello, H. Ariga, M. G. Musolino, R. Pietropaolo, S. Takakusagi, K. Asakura, Appl. Catal., B 166 (2015) 121−133.

[31] M. G. Musolino, C. Busacca, F. Mauriello, R. Pietropaolo, Appl. Catal., A 379 (2010) 77−86.
[32] M. G. Musolino, L. A. Scarpino, F. Mauriello, R. Pietropaolo, ChemSusChem 4 (8) (2011) 1143−1150.
[33] International Center for Diffraction Data, Powder Diffraction Database, Penn- sylvania, PA, 1997.
[34] B. A. Sexton, A. E. Hughes, T. W. Turney, J. Catal. 97 (1986) 390-406.
[35] L.S.F. Feio, C.E. Hori, L.V. Mattos, D. Zanchet, F.B. Noronha, J.M.C. Bueno, App. Catal. A: Gen. 348 (2008) 183–192.
[36] F.B. Noronha, M. Schmal, C. Nicot, B. Moraweck, R. Fréty, J. Catal. 168 (1997) 42–50.
[37] M.L. Cubeiro, J.L.G. Fierro, J. Catal. 179 (1998) 150–162.
[38] Y-S. Fenga, X-Y. Lina, J. Haoa, H-J. Xu, Tetrahedron 70 (2014) 5249-5253.
[39] C.D. Wanger, W.M. Riggs, L.E. Davis, J.F. Moulder, G.E. Muilenberg, Handbook of X-ray Photoelectron Spectroscopy, Perkin-Elmer Corp., Minnesota, USA, 1979.
[40] B. Mierzwa, Z. Kaszkur, B. Moraweck, J. Pielaszek, J. Alloys Compd 286 (1999) 93–97.
[41] L. Nguyen, S. Zhang, L. Wang, Y. Li, H. Yoshida, A. Patlolla, A.I. Frenkel, S. Takeda, F.F. Tao, ACS Catal. 6 (2) (2016) 840–850.
[42] E. Dorrestijn, L. J. J. Laarhoven, I. W. C. E. Arends, P. Mulder, J. Anal. Appl. Pyrolysis 54 (1−2) (2000) 153−192.
[43] R. Parthasarathi, R. A. Romero, A. Redondo, S. Gnanakaran, J. Phys. Chem. Lett. 2 (20) (2011) 2660−2666.

**Figure captions**

**Scheme 1.** Benzyl Phenyl Ether (BPE), 2-Phenethyl Phenyl Ether (PPE) and Diphenyl Ether (DPE): the simplest lignin-derived aromatic ethers.

**Figure 1.** XRD profiles of unreduced (down) and reduced (up) Pd/Co catalyst.

**Figure 2.** SEM-EDX characterization of Pd/Co catalyst.

**Figure 3.** TEM image and relative metal particle size distribution of Pd/Co catalyst.

**Figure 4.** $H_2$-TPR profiles of unreduced Pd/Co and $Co_3O_4$ catalysts

**Figure 5.** XPS plots of the reduced Pd/Co catalyst in Co $2p_{3/2}$ and Pd $3d_{5/2}$ levels

**Figure 6.** Product yields in the conversion of BPE with the Pd/Co catalyst under transfer hydrogenolysis conditions at 210°C against time (reaction conditions: 0.125 g of catalyst; 40 ml solution of BPE 0.1 M; time: 180 minutes; $N_2$ pressure: 10 bar; stirring: 500 rpm).

**Figure 7.** Recycling tests for Pd/Co catalyst in the CTH of BPE at 240°C

**Figure 8.** Conversion in the CTH and in the hydrogenolysis of BPE, PPE, and DPE at 240°C (reaction conditions: 0.125 g of catalyst; 40 ml solution of BPE 0.1 M; time: 180 minutes; $N_2$ or $H_2$ pressure: 10 bar; stirring: 500 rpm)

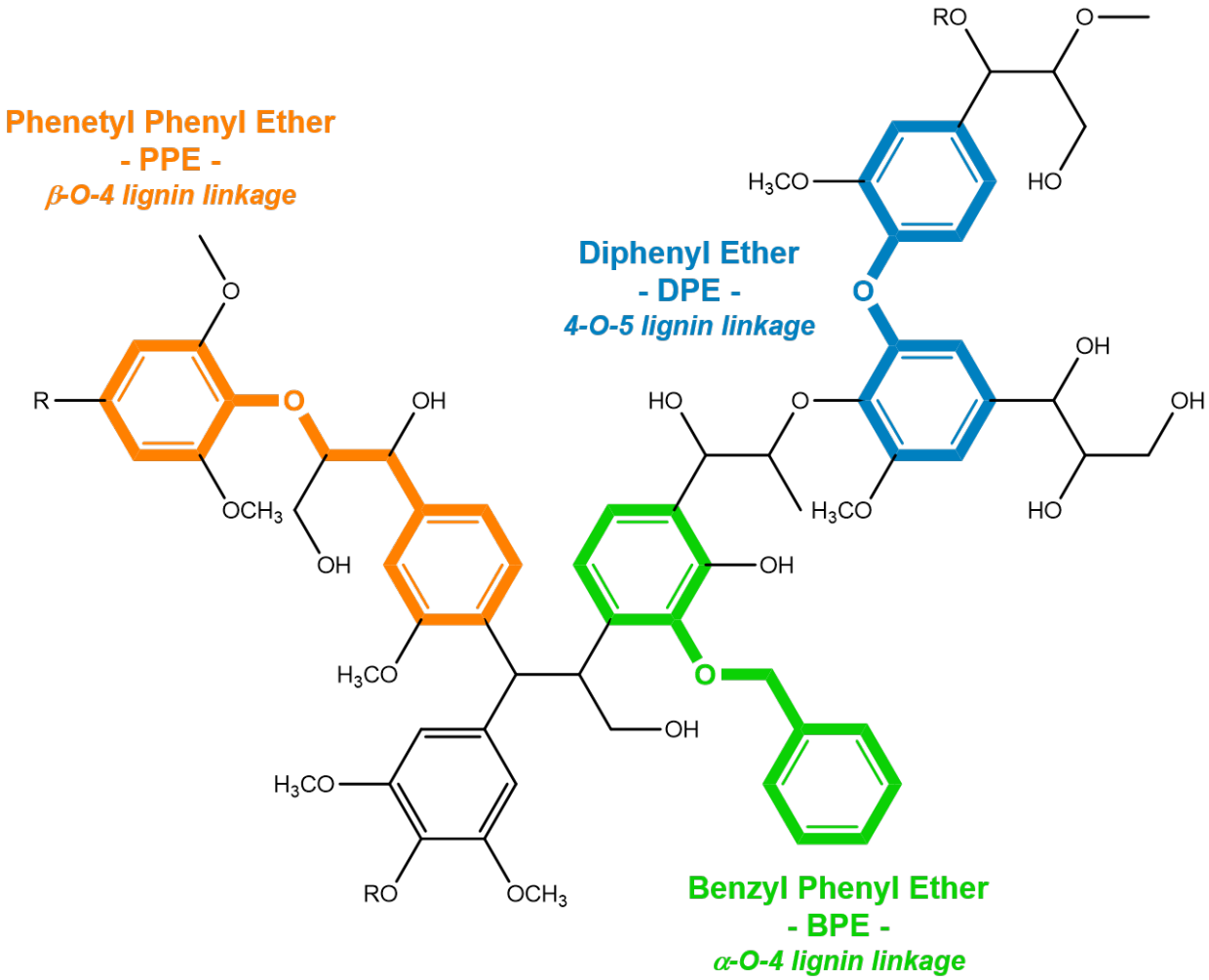


**Scheme 1** Benzyl Phenyl Ether (BPE), 2-Phenethyl Phenyl Ether (PPE) and Diphenyl Ether (DPE): the simplest lignin-derived aromatic ethers.

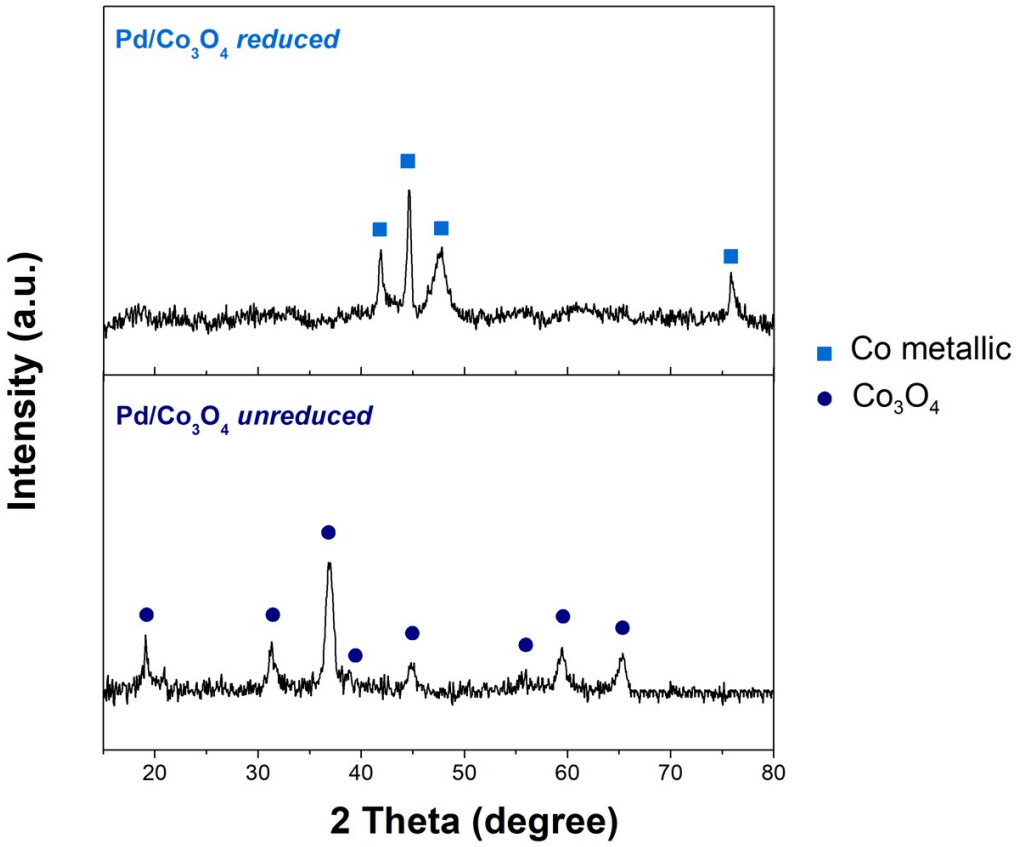


**Figure 1** XRD profiles of unreduced (down) and reduced (up) Pd/Co catalyst.

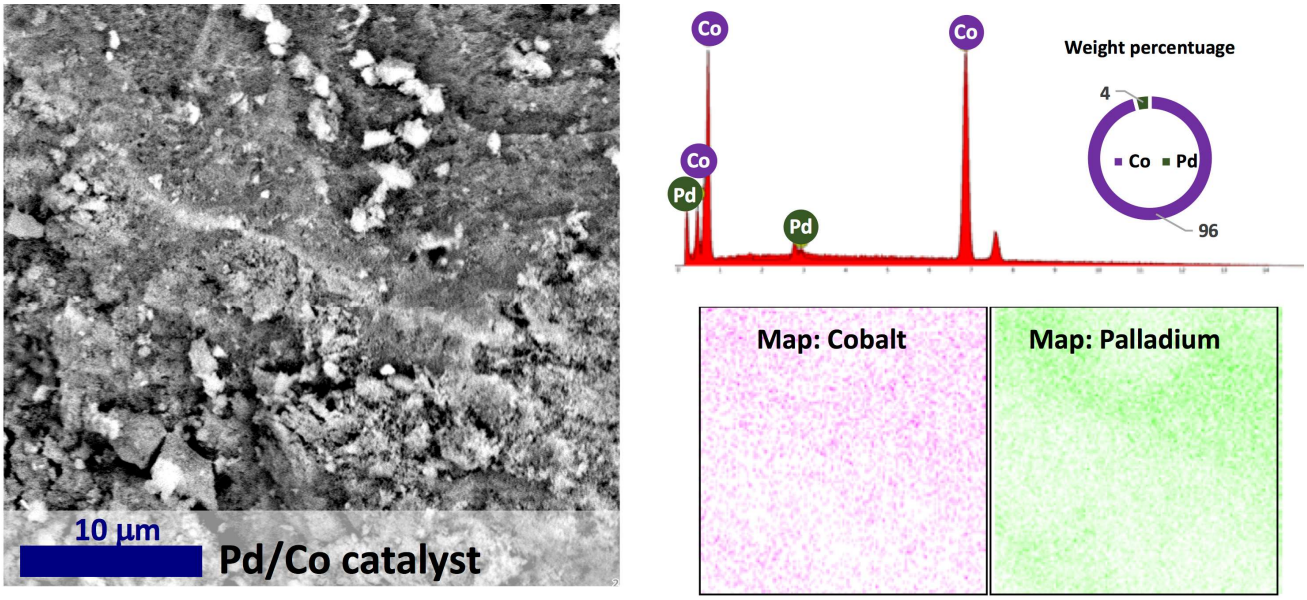


**Figure 2** SEM-EDX characterization of Pd/Co catalyst.

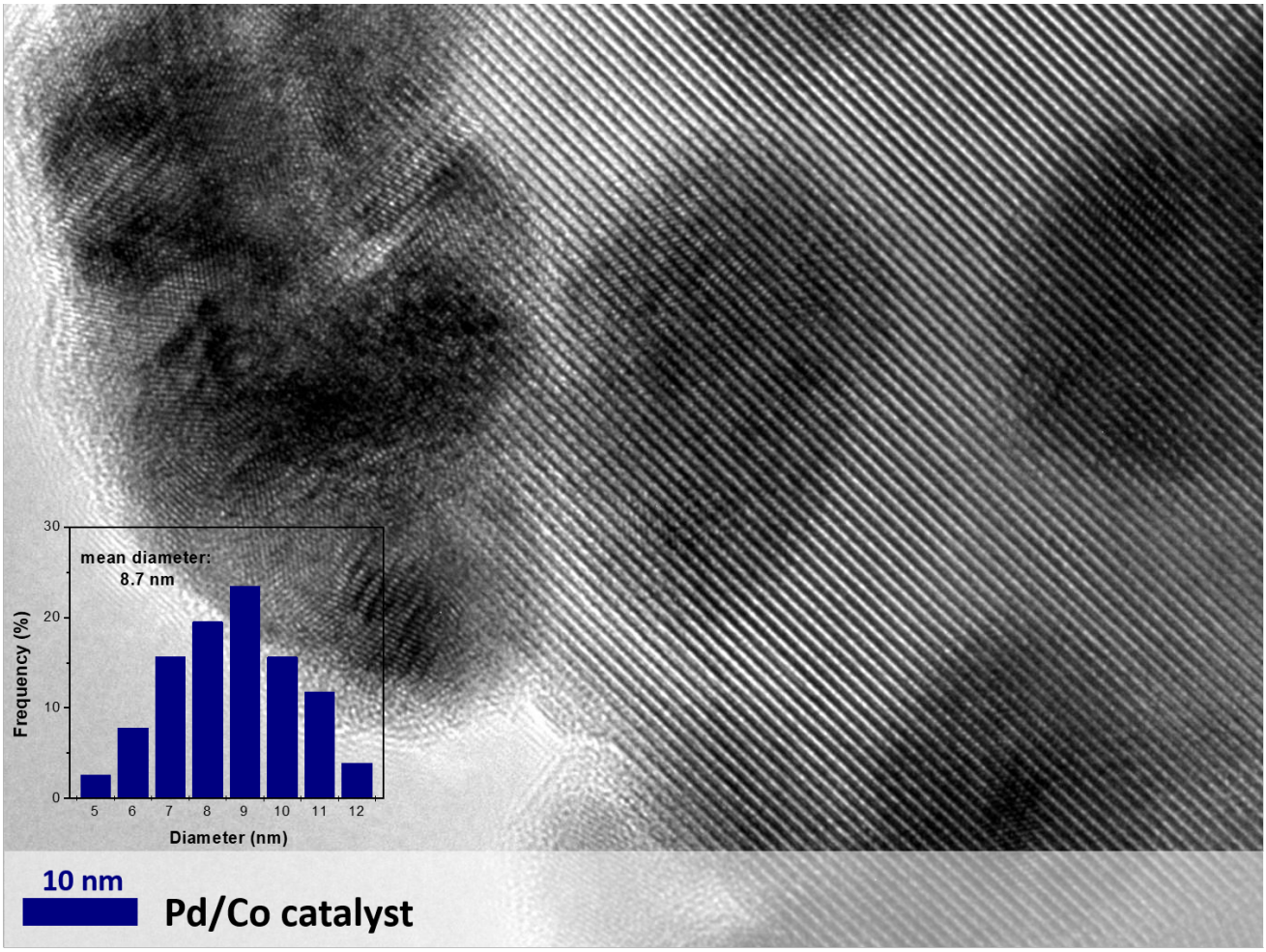


**Figure 3** TEM image and relative metal particle size distribution of Pd/Co catalyst.

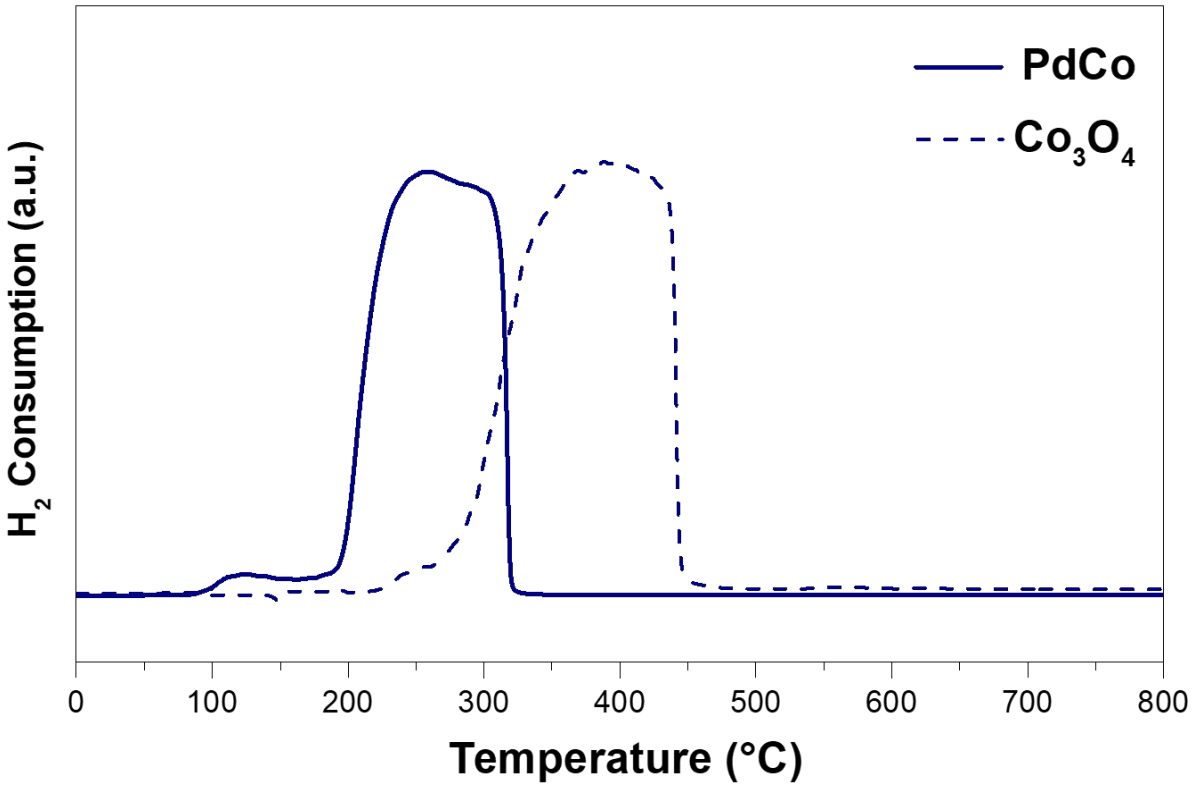


**Figure 4** $H_2$-TPR profiles of unreduced Pd/Co and $Co_3O_4$ catalysts

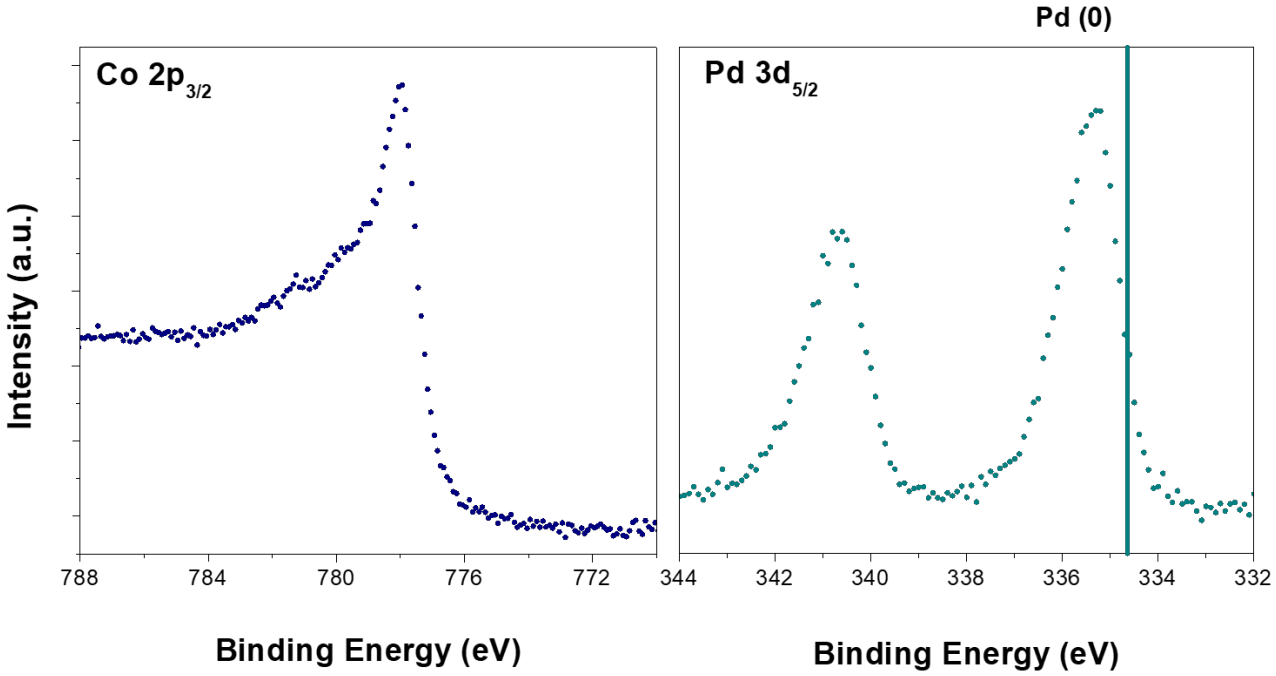


**Figure 5** XPS plots of the reduced Pd/Co catalyst in Co $2p_{3/2}$ and Pd $3d_{5/2}$ levels

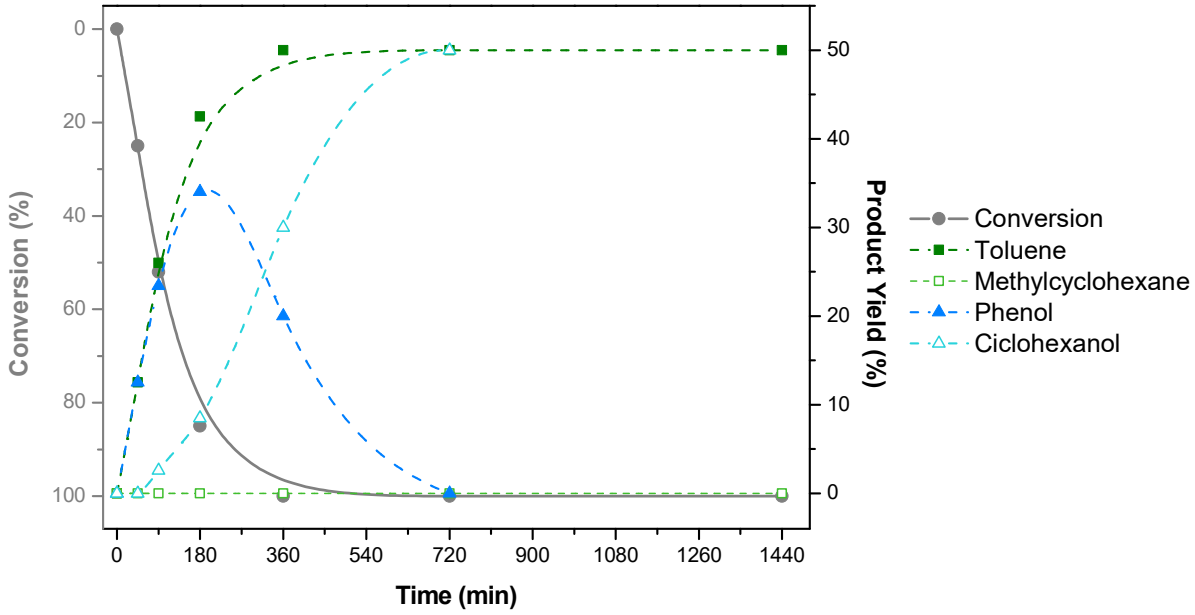


**Figure 6.** Product yields in the conversion of BPE with the Pd/Co catalyst under transfer hydrogenolysis conditions at 210°C against time (reaction conditions: 0.125 g of catalyst; 40 ml solution of BPE 0.1 M; time: 180 minutes; $N_2$ pressure: 10 bar; stirring: 500 rpm).

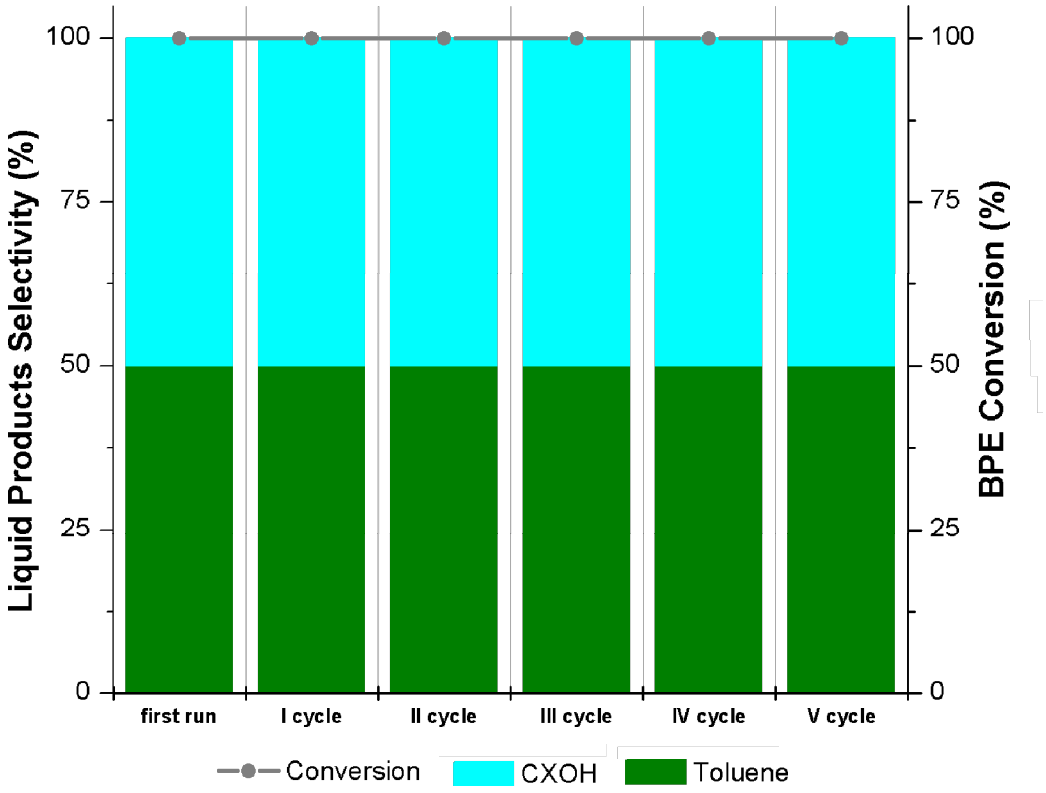


**Figure 7.** Recycling tests for Pd/Co catalyst in the CTH of BPE at 240°C

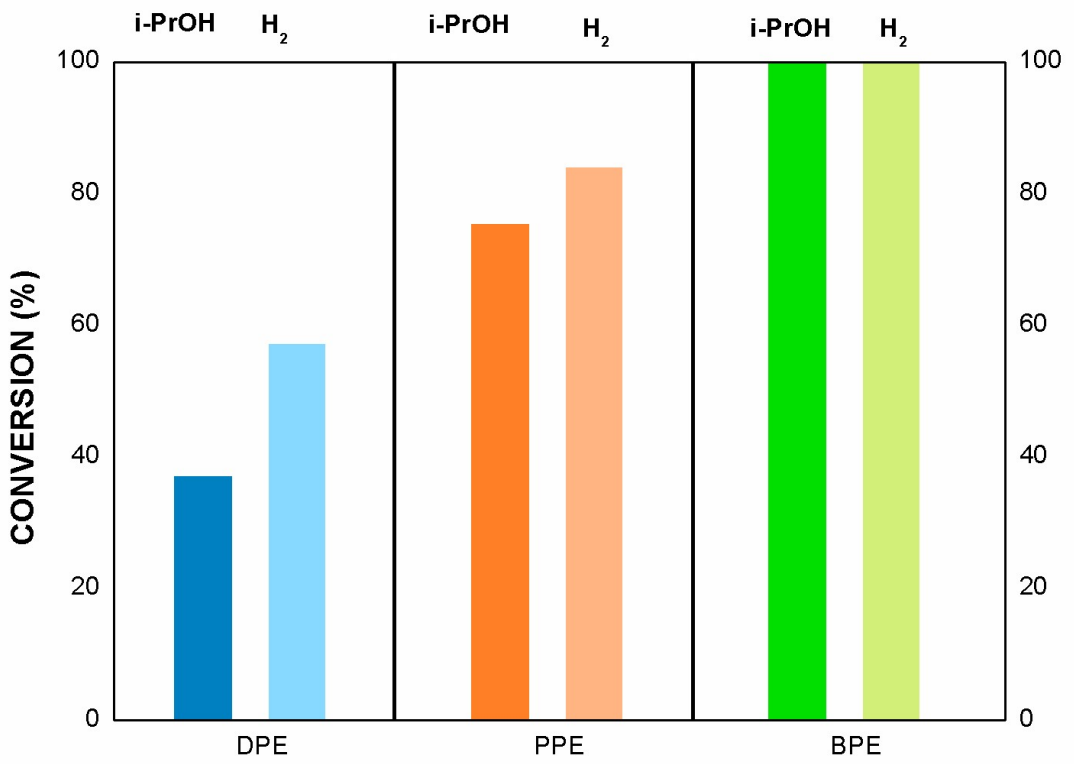


**Figure 8.** Conversion in the CTH and in the hydrogenolysis of BPE, PPE, and DPE at 240°C (reaction conditions: 0.125 g of catalyst; 40 ml solution of BPE 0.1 M; time: 180 minutes; $N_2$ or $H_2$ pressure: 10 bar; stirring: 500 rpm)

**Table 1**. Main characteristic of Ni and PdNi catalysts

| **Catalyst notation** | **S.A. [$m^2$/g]** | **Pd loading [%]** | **Pd $d_n$ [nm]** |
|---|---|---|---|
| Pd/Co | 105 | 4.4 | 8.7 |

***S.A:*** *surface area;* ***Pd loading [%]:*** *amount of palladium as determined by X-ray fluorescence (XRF) analysis;* ***Pd $d_n$ [nm]:*** *palladium mean particles size from TEM.*

**Table 2**. X-ray absorption fine structure characterization at the Pd K-edge for Pd/Co catalyst.

| **Catalyst** | **Scattering Pair** | **CN** | **R (Å)** | **DW (Å)** | **R** |
|---|---|---|---|---|---|
| Pd/Co | Pd-Pd | 0,9 | 2,69 | 0,021 | 0,02 |
| | Pd-Co | 3,9 | 2,51 | 0,047 | |

***CN:*** *Coordination number;* ***R:*** *Interatomic distance;* ***DW:*** *Debye–Waller factor*

**Table 3**. Transfer hydrogenolysis of benzyl phenyl ether (BPE) in the presence of Pd/Co and Pd/C catalysts by using 2-propanol as H-source (reaction conditions: 0.125 g of catalyst; 40 ml solution of BPE 0.1 M; time: 180 minutes; $N_2$ pressure: 10 bar; stirring: 500 rpm)

| Catalyst | Temperature [°C] | Conversion [%] | Chemoselectivity [%] | | | | Aromatic Yield [%] |
|---|---|---|---|---|---|---|---|
| | | | TOL | MCX | PHE | CXO | |
| Pd/Co | 240 | 100 | 50 | - | - | 50 | 50 |
| Pd/C | 240 | 45 | 50 | - | 40 | 10 | 41 |
| Pd/Co | 210 | 88 | 50 | - | 43 | 7 | 82 |
| Pd/C | 210 | 18 | 50 | - | 50 | - | 18 |
| Pd/Co | 180 | 30 | 50 | - | 50 | - | 30 |
| Pd/C | 180 | - | - | - | - | - | - |

***TOL**: Toluene; **MCX**: Methylcyclohexane; **PHE**:Phenol; **CXO**: Cyclohexanol*